Development of an Automated Microinjection System for Fabrication of Carbon Nanotube Sensors

Selina C. Qu, Carmen K. M. Fung, Rosa H. M. Chan and Wen J. Li*
Centre for Micro and Nano Systems
The Chinese University of Hong Kong
Hong Kong SAR

**Contacting Author: wen@acae.cuhk.edu.hk*
Phone: +852 2609 8475 Fax: +852 2603 6002

***Abstract* – A novel automated Carbon Nanotube (CNT) microinjection system for batch fabricated a bulk multi-walled carbon nanotubes (MWNT) based MEMS sensor is presented. The basic process includes AC electrophoretic manipulation of MWNT bundles on a silicon substrate and embedding them inside parylene C layers to provide a robust protection for the bundled MWNT. By utilizing AC electrophoretic technology, CNTs were successfully and repeatably manipulated between micro-fabricated electrodes. Besides, the devices were demonstrated to potentially serve as novel thermal sensors with low power consumption (~ μW) and fast frequency response (~ 100 kHz). Based on these experimental evidences, a feasible batch manufacturable method for functional CNT sensors by using the automated injection system is developed which will dramatically reduce production costs and production time of nano sensing devices and potentially enable fully automated assembly of CNT based devices.**

1. INTRODUCTION

Carbon nanotubes (CNTs), since discovered in 1991 by Sumio Iijima [1], have been extensively studied for their electrical (e.g., see [2]) and mechanical properties (e.g., see [3]). Owing to their minute dimensions, good mechanical and electrical properties, different groups started to utilize CNTs as nano sensors or actuators for different applications in nanoelectronic or nano-electro-mechanical systems (NEMS). In order to build a CNT based device, fast and batch techniques to manipulate the CNT has to be developed. Typical manipulation technique is by atomic force microscopy [4]. However, this pick-and-place technique is time consuming, though the technique has very high positioning accuracy. Past demonstrations by K. Yamamoto et al. showed that carbon nanotube can be manipulated by AC and DC electric field [5][6]. Besides, a recent report from L. A. Nagahara et al. demonstrated the individual single-walled carbon nanotube (SWNT) manipulation using nano-electrodes by AC bias voltage [7]. By using similar technique (i.e., AC electrophoresis), we have successfully manipulated bundled carbon nanotubes to form resistive elements between Au microelectrodes for sensing and electronic circuits efficiently. However, in our prior work, we found that the yield of the batch assembly of the CNT devices cannot be 100% as the volume of each drop of the CNTs/ethanol solution during the CNT manipulation can be varied. Therefore, in order to improve the yield, a precise and automated CNT injection system is developed. This paper reports the technique to form bundled MWNT resistive element between Au electrodes. In addition, a MEMS-compatible process to encapsulate the MWNT bundles for reliable measurements and our preliminary experimental findings on the electrical characterizations such as frequency response and I-V characteristics of the bundled MWNT sensors are also presented. Besides, the preliminary CNT microinjection system will be presented. The results indicate that the carbon nanotube is promising to be used as high performance and low power consumption devices for future electronic and sensing applications.

2. FORMATION OF CNT ELEMENTS BY AC ELECTROPHORESIS

2.1 AC Electrophoretic Manipulation of CNT

2.1.1 Theoretical Background and Modeling

AC electrophoresis (or dielectrophoresis) is a phenomenon where neutral particles undergoing mechanical motion inside a non-uniform AC electric field (see Figure 1). Detailed descriptions on AC electrophoresis can be found in [8].

In our CNTs manipulation experiments, CNTs were dispersed inside a liquid medium (e.g., ethanol), therefore other forces (e.g., viscous force), other than the dielectrophoretic forces, are also imparted on CNTs during the manipulation process. In order to understand the physical phenomenon during the dielectrophoretic manipulation, we have conducted the following simulations with experimental verifications on the effect of a pair of microelectrodes on CNT alignments.

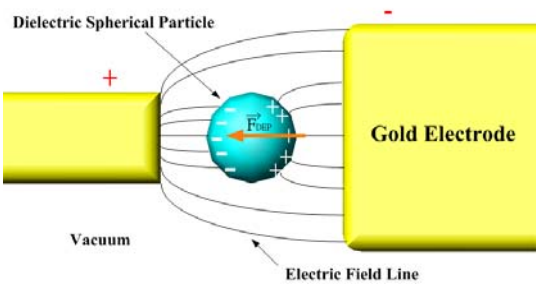

Figure 1. Under non-uniform AC electric field, dielectrophoretic force induced on the neutral particles cause mechanical motion on the particles.

With negligible gravitational force, the three main force components are the dielectrophoretic (DEP) force, the viscous force and the electro thermal force. For other small particles with their volumes compatible to MWNT, the thermal effects can dominate, but the high polarizability of MWNT makes the DEP force large enough to produce the deterministic movements.

Dielectrophoresis refers to the force exerted on a polarized particle in a non-uniform electric field [8][9]. It can be written as

$$\boldsymbol{F}_{\boldsymbol{DEP}}(t) = (\boldsymbol{m}(t)\cdot\nabla)\boldsymbol{E}(t) \qquad (1)$$

where E is the electric field, m is the induced dipole moment of MWNT. Assumed that the MWNT is a long prolate spheroid with the longest axis aligned with the electric field, the induced dipole moment is

$$\boldsymbol{m}(t) = 4\pi\varepsilon_m ab^2 K\boldsymbol{E}(t) \qquad (2)$$

where ε_m, K, a and b are the absolute permittivity of the medium, the complex polarization factor, the half length of MWNT and the radius of MWNT, respectively. Since the electric field components are in phase, the time averaged DEP force deduced from the above equations is

$$< \boldsymbol{F}_{\boldsymbol{DEP}}(t) >= 2\pi ab^2\varepsilon_m \,\mathrm{Re}(K)\nabla \mid \boldsymbol{E}_{rms} \mid^2 \qquad (3)$$

where $\nabla \mid \mathrm{E}_{rms} \mid^2$ is the gradient of the square of the root-mean-square of the electric field.

An array of microelectrodes is fabricated and the CNT connections across the microelectrodes by the dielectrophoresis are shown in Figure 2. Details of the experimental procedures for the dielectrophoretic manipulation of MWNT will be presented in the next section. On the other hand, in order to visualize the electric field distribution generated by pairs of microelectrodes, simulations have been conducted and described in the following part.

The approximate order of the potential was investigated by using Green's theorem [10], and the square root-mean-square magnitude of the field was calculated by using MatLab. Since the magnitude of the electric field decreases with height from the electrodes, the positive DEP draws the MWNT downwards to the edges of the electrodes. The force fields in Figure 3 are estimated by (3), assuming that the longest axes of MWNT is parallel to the instantaneous electric field.

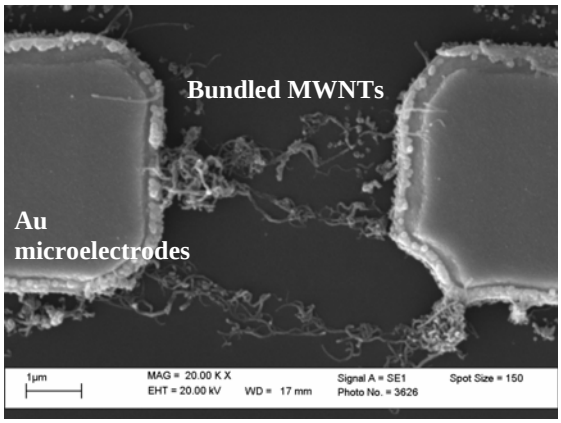

Figure 2. Scanning electron microscopic (SEM) image showing the MWNT connections between Au microelectrodes.

Downward forces are shown by the contours in Figure 3 between the electrodes and close to the electrode surfaces. The DEP forces are significantly large to draw the MWNT downwards and to overcome the upward movement from the electro thermal effect [11].

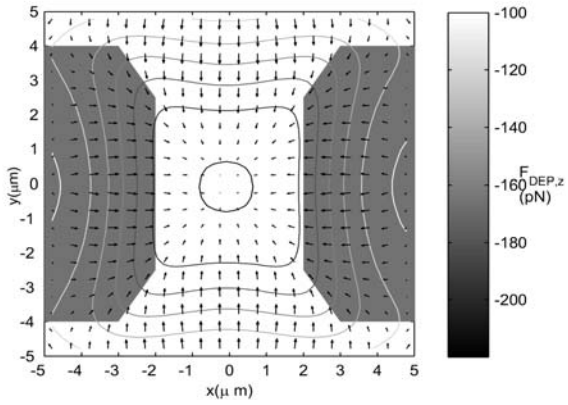

Figure 3. Average DEP force between the electrodes which were applied by the 16V peak-to-peak AC voltage at 1MHz. The arrows are the force vectors on x-y plane at 3 μm above electrodes in Figure 2.The contours represent the order of downward forces.

2.1.2 Experimental Details

The bundled MWNT used in the experiments were ordered commercially from [12] (prepared by chemical vapour deposition). The axial dimension and the diameter of the MWNT was 1 – 10 μm and 10 – 30 nm, respectively. Prior to the MWNT manipulation, 50 mg of the sample was ultrasonically dispersed in 500 mL ethanol solution and the resulting solution was diluted to 0.01 mg/mL for later usage.

After the Au microelectrodes were fabricated as described in [13], the silicon substrate with arrays of sensor-electrodes was place on the vacuum-pump stage of a micromanipulator station. Then approximately 10 μL of the MWNT/ethanol solution was transferred to the substrate by 6 mL gas syringe (see Figure 4) and the Au microelectrodes were excited by AC voltage source (typically, 16 V peak-to-peak at 1 MHz). The ethanol was evaporated away leaving the MWNT to reside between the gaps of the microelectrodes (see Figure 2). To test the connectivity of MWNT to the electrodes for each sensor, room temperature resistances between the microelectrodes were measured before the sensors were advanced to the next fabrication procedure and the two probe room temperature resistances of the samples typically range from several kΩ to several hundred kΩ.

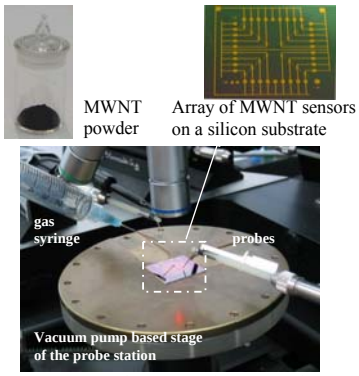

Figure 4. Experimental setup for CNT manipulation to build MWNT sensors.

3. PARYLENE/CNT/PARYLENE EMBEDDED MWNT SENSORS

3.1 Fabrication Process

The fabrication process for the parylene embedded CNT sensor is shown in Figure 5. We are currently fabricating the MWNT based MEMS sensors for different sensing purposes. In order to protect the bundled MWNT from contaminates and to avoid their detachment from the electrodes, a parylene C polymer is used to embed the bulk MWNT. The advantage of using Paraylene C is that it can be deposited conformally at room temperature. As seen in the fabrication process, SiO_2 was first deposited on the silicon substrate to avoid conduction of the gold electrode with the substrate. Then the Au and Cr microelectrodes were patterned on the substrate (Cr was used to improve the adhesion of Au to the substrate). It provides a small gap distance to allow the CNT manipulation more efficiently. This gap distance for the CNT sensor is between 3μm and 10μm. The bottom parylene C layer was then deposited on the substrate to isolate the MWNT bundles from the substrate. Based on the technique for CNT manipulation presented in the pervious section, the bulk MWNT was manipulated and connected across the microelectrodes of each sensor (by observing the resistance change between the electrodes). Finally, the top parylene C layer was deposited to embed the MWNT and protect them from contamination. An optical microscopic image of the fabricated MWNT sensor is shown in Figure 6.

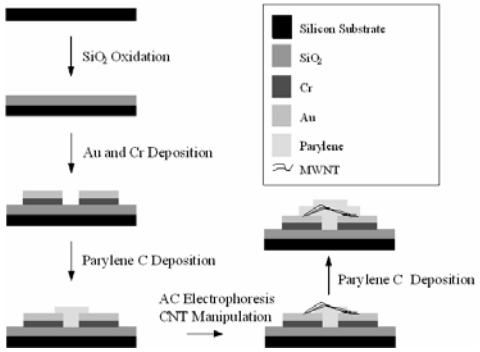

Figure 5. Fabrication process flow for the CNT based MEMS Sensor.

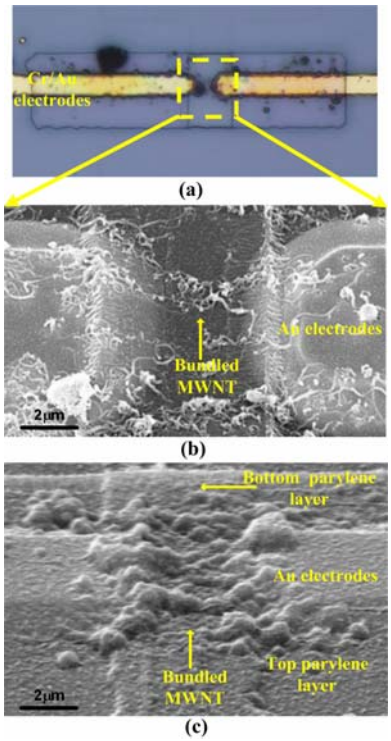

Figure 6. (a) Optical microscopic image showing the prototype parylene/MWNT/parylene sensor, (b) and (c) Scanning electron microscopic (SEM) images showing the bulk MWNT form on the top of the parylene C layer and were embedded inside the parylene C layers respectively.

4. EXPERIMENTAL RESULTS

We have investigated the possibility to utilize the bundled CNTs as sensing elements for thermal sensing. Comparing to the results collected for the un-encapsulated MWNT devices reported in [13] and [14], the resistance for these embedded CNT sensors is more stable and consistent. We have also proved that these embedded based MEMS sensors have ultra low power consumption and high frequency response. Details of the experimental results are discussed in this section.

4.1 Thermal Sensitivity

The bundled MWNT as sensing elements for micro thermal sensors can be driven in constant current mode configuration (see Figure 7). An experiment for investigating the temperature dependence of the bulk MWNT sensor was performed. The fabricated sensor chip was packaged on a PCB for data acquisition and was put inside an oven. Then, the resistance change of the MWNT sensors was measured as the temperature inside oven was varied. The temperature-resistance relationship for the MWNT sensors was measured and a representative data set is shown in Figure 8 for several cycles of measurements. From the experimental results, the bundled MWNT resistance dropped with temperature, which is in agreement with [15]. Other than the first measurement cycle, the resistance at room temperature converged and the slopes are consistent for each measurement. The temperature-resistance dependency of bundled MWNT implied its thermal sensing capability. By observing the drift in resistance for the first measurement, we concluded that the MWNT sensors become stable after a temperature annealing process. Based on experimental results, the range of the temperature coefficient of resistance (TCR) for the MWNT sensors was found to be from -0.04 to -0.07 $\%/^{o}C$.

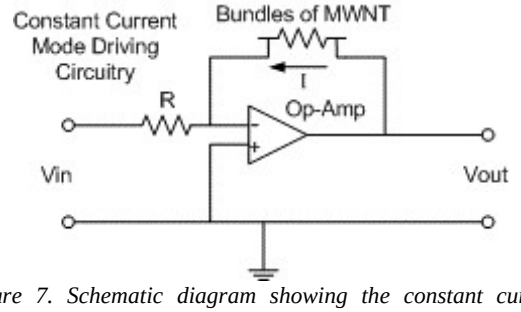

Figure 7. Schematic diagram showing the constant current mode circuit used in our experiments.

By comparing the drift in the room temperature resistance and convergence of data from measurement of different temperature ramping cycles reported in [13] and [14], the performance of current parylene encapsulated MWNT sensors are more stable and consistent. With parylene protecting the MWNT linkage between the microelectrodes, these new MWNT based MEMS sensors will have much less contaminations such as moisture and dust particles during measurements, and also will not have MWNT detaching from the Au electrodes even if the sensors undergo thermal cycling.

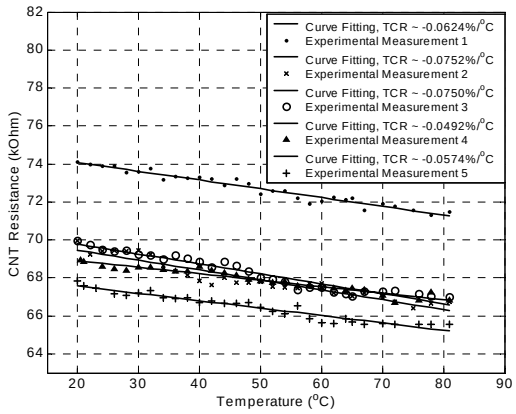

Figure 8. TCR for a Parylene/MWNT/Parylene sensor in five different measurements.

4.2 Power Consumption

The I-V Characteristic of the MWNT sensors was also investigated. From the results of experiments conducted on two different MWNT sensors, the current required to induce self heating of the MWNT devices was in μA range at several volts which suggests that the power consumption of these devices is in μW range (see Figure 9).

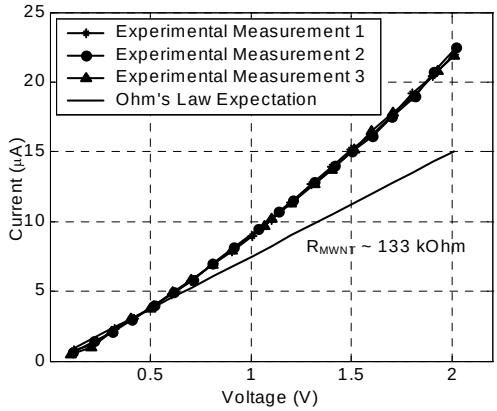

Figure 9. I-V characteristics of a Parylene/MWNT/Parylene sensor. Three repeated measurements were performed to validate its repeatability. The straight line is the theoretical expectation using Ohm's Law. The room temperature resistance of bundled MWNT of this sample was about 310 kΩ .

4.3 Frequency Response

Investigation on the frequency response of the MWNT sensor was also carried out. To test the frequency response of the embedded bundled MWNT sensor, input square wave of 3 V peak-to-peak at 19 kHz was fed into the negative input terminal of the circuit shown in Figure 7 and the output response was observed on an oscilloscope (see Figure 10). From our experimental measurements, bundled MWNT sensors exhibited very fast frequency response (about 148 kHz). As a comparison, typical frequency response of MEMS polysilicon sensors in constant current mode configuration without frequency compensation is around several hundred Hz to several kHz [16][17].

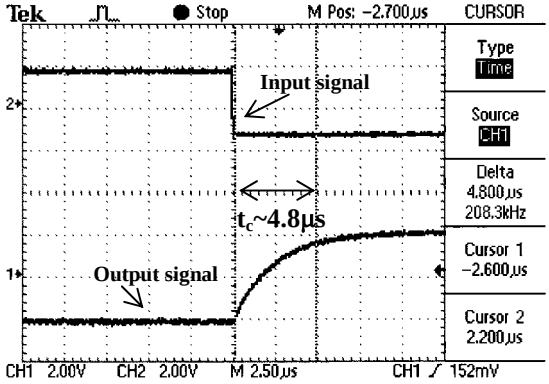

Figure 10. Frequency response of MWNT bundles in constant current mode.

5. AUTOMATED CNT MICROINJECTION SYSTEM

Based on the results of CNT formation by using AC electrophoresis process and the thermal sensing capability of the bundled CNT sensor, we are now developing a computer-controlled CNT microinjection system for performing the dielectrophoresis CNT manipulation automatically. The preliminary prototype architecture of the CNT microinjection system is shown in Figure 11. It mainly consists of three parts: motorized manipulators, a set of video microscope system, and a computer. A chip with sensors-microelectrodes and the ethanol/CNT solution are placed on an x-y motorized plate. A nano probe fabricated in [18] is fixed on another manipulator and moves in z direction, which is used to transfer the solution on the microelectrodes. In order to obtain an image data of the chip, a video microscope is fixed on a manual manipulator and a mirror are used to observe the position of the microelectrodes in the chip.

Prior to the experiment, a pre-adjustment of the microscope system is performed to make the microscope coordinate frame consistent with the x-y-z stage coordinate frame. Firstly, the nano probe with the z-stage is commanded to move downwards to give a drop on the chip, and move it upwards to the start position. Afterwards, the microscope and the mirror are adjusted to locate the drop clearly in the center of the monitor. Therefore, the projection of the nano probe on the chip is exactly observed in the center of the monitor for the latter stage of the experiment.

As described before, the main procedure of the experiment is to couple the solution sample to the chip, which is controlled by the computer program automatically. A program is developed to read the image data of the monitor which is obtained in the pre-adjustment stage, and to determine the position of a pair of microelectrode, then the chip with the x-y stage is moved to make the pair of microelectrodes is exactly at the center of the monitor. Then the nano probe is controlled to move downwards to drop the solution exactly in the gap of the microelectrodes. The same operation is done repeatedly until all microelectrodes in the chip are dropped by the solution.

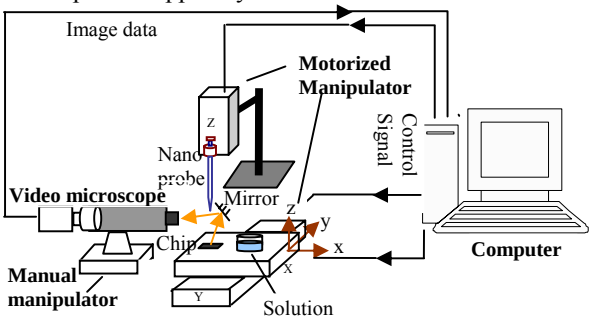

Figure 11. The architecture of the CNT microinjection system.

6. CONCLUSION

A technique to form encapsulated bundled MWNT resistive elements between Au electrodes was presented. The TCR measurements and the frequency response measurement of the bundled MWNT based MEMS sensors showed that bundled MWNT can be used as a sensing element for high performance, i.e., ultra-low-power and high-frequency-response thermal sensing applications. Also, by embedding the MWNT bundles inside parylene C polymer layers, the stability of the sensor increased. Moreover, the operating power of the resulting devices is in the µW range, which is ultra low power consumption for applications such as fluidic shear-stress sensing or thermal imaging.

7. ACKNOWLEDGEMENTS

Funding for this project was provided by The Chinese University of Hong Kong (CUHK). The authors would like to sincerely thank Dr. W.Y. Cheung of the Department of Electronic Engineering of CUHK and Mr.

Victor T. S. Wong of the Department of Mechanical and Aerospace Engineering of University of California for their help and discussion on this project.

8. REFERENCES

[1] S. Iijima, “Helical microtubules of graphitic carbon”, Nature, Vol. 354, pp. 56 – 58, 1991.

[2] S. Frank, P. Poncharal, Z.L. Wang, W.A. de Heer, “Carbon nanotube quantum resistors”, Science, Vol. 280, pp. 1744 – 1746, 1998.

[3] E.W. Wong, P.E. Sheehan, C.M. Lieber, “Nanobeam mechanics: elasticity, strength, and toughness of nanorods and nanotubes”, Science, Vol. 277, pp.1971 – 1975, 1997.

[4] T. Shiokawa, K. Tsukagoshi, K. Ishibashi, Y. Aoyagi, “Nanostructure construction in single-walled carbon nanotubes by AFM manipulation”, Microprocesses and Nanotechnology Conference 2001, pp. 164 – 165, 2001.

[5] K. Yamamoto, S. Akita, Y. Nakayama, “Orientation of carbon nanotubes using electrophoresis”, Japanese Journal of Applied Physics, Vol.35, L917-L918, 1996.

[6] K. Yamamoto, S. Akita, Y. Nakayama, “Orientation and purification of carbon nanotubes using AC electrophoresis”, Journal of Physics D: Applied Physics, Vol. 31, L34-L36, 1998.

[7] L.A. Nagahara, I. Amlani, J. Lewenstein and R.K. Tsui, “Directed placement of suspended carbon nanotubes for nanometers-scale assembly”, Applied Physics Letters, Vol. 80, No. 20, pp. 3826 – 3828, 2002.

[8] H.A. Pohl, “Dielectrophoresis: The behaviour of neutral matter in nonuniform electric fields”, Cambridge University Press, 1978.

[9] T. B. Jones, “Electromechanics of particles”, Cambridge: Cambridge University Press, 1995.

[10] X. Wang, X-B Wang, F. F. Becker, and P. R. C. Gascoyne, “A theoretical method of electrical field analysis for dielectrophoretic electrode arrays using Green’s theorem”, J. Phys. D: Appl. Phys., Vol. 29, pp.1649 – 1660, 1996.

[11] T. Heida, W. L. C. Rutten, and E. Marani, “Understanding dielectrophoretic trapping of neuronal cells: modeling electric field, electrode-liquid interface and fluid flow”, J. Phys. D: Appl. Phys., Vol. 35, pp.1592 - 1602, 2002.

[12] Sun Nanotech Co Ltd, Beijing, P.R. China.

[13] Victor T. S. Wong and Wen J. Li, "Bulk carbon nanotubes as sensing element for temperature and anemometry micro sensing", IEEE MEMS 2003, pp.41 – 44, 2003.

[14] Victor T. S. Wong and Wen J. Li, "Bundled carbon nanotubes as electronic circuit and sensing elements", IEEE ICRA 2003, Vol. 3., pp.3648 –3653, 2003.

[15] T.W. Ebbesen, H.J. Lezec, H. Hiura, J.W. Bennett, H.F. Ghaemi, T. Thio, “Electrical conductivity of individual carbon nanotubes”, Nature, Vol. 382, pp. 54 – 56, 1996.

[16] C. Liu, J.B. Huang, Z. Zhu, F. Jiang, S. Tung, Y.C. Tai, C.M. Ho, “A micromachined flow shear-stress sensor based on thermal transfer principle”, Journal of Microelectromechanical Systems, Vol. 8, No. 1, pp. 90 – 99, 1999.

[17] J.B. Huang, F.K. Jiang, Y.C. Tai, C.M. Ho, “MEMS-based thermal shear-stress sensor with self-frequency compensation”, Measurement Science and Technology, Vol. 10, No. 8, pp. 687 – 696, 1999.

[18] K.W.C. Lai, W.J. Li, “KL probes for robotic-based cellular nano surgery”, IEEE Nano 2003, Vol. 1, pp. 152 – 155, 2003.